



Inversion of data from Laser Ultrasonic Characterization of Hot-Rolled Steel Strip

A. Volker¹, A. Duijster¹, D. Krix², R. Schmidt³, F. van den Berg⁴

¹ TNO, The Netherlands, arno.volker@tno.nl

² Salzgitter Mannesmann Forschung GmbH, Germany, d.krix@du.szmf.de

³ Arcelor-Mittal Eisenhüttenstadt, Germany, rene.schmidt@arcelormittal.com

⁴ Tata Steel, The Netherlands, frenk.van-den-berg@tatasteel.com

Abstract

Grain size and texture are important properties of sheet metal because they greatly influence the mechanical properties. Laser ultrasonic measurements offer the potential to monitor the product uniformity inline. The grain size is known to affect ultrasonic attenuation by scattering on grain boundaries, and texture influences the velocity of the propagated waves in different directions. Measuring the attenuation inline poses some challenges because of the thin sheet thickness and relatively small grains. A new approach is proposed by measuring the full ultrasonic wave field along a line at the surface of the sample using non-contact laser-based generation and detection methods. Analysis of multiple wavefronts in the data leads to information about the texture of a sample. The data is also analysed by double Fourier transform in the wavenumber-frequency domain, where specific parts of the observed dispersion curves can be associated with pure compressional and shear waves. The energy distribution as function of mode number is used to characterize different samples in the rolling and transverse direction. The method is applied to various steel grades from different manufacturers, and influences of grain size and/or texture variations are shown.

1. Introduction

Flat products for the automotive and packaging industries need to have favourable forming properties to press the steel sheets in the desired shape, with minimal risk on tearing, ductile fracture, earing and springback. Therefore, it is of utmost importance to control, during the manufacturing of steel strip, the relevant mechanical properties like yield strength (R_p), tensile strength (R_m), Lankford coefficient (r) and planar anisotropy coefficient or planar R -value.

These mechanical properties are governed by the microstructure, in particular (but not exclusively) by the grain size and the distribution of the orientation of the crystallites (texture). Laser-based UltraSonics (LUS) (1) is a technique with which information can be gained on the grain size and the texture in real-time and contact-free on moving material. Hence, it has potential to be applied inline during the production of steel strip.

The LUS technique employs a powerful pulse laser to generate, via the mechanism of ablation, high-frequency ultrasonic pulses into the material under test. A second, continuous wave laser is used to detect the deviation of the material surface due to the (reflected) waves. The propagation and the degree of scatter of the ultrasonic waves in matter are influenced by the grain size and texture. Hence, LUS may provide a direct probe to the microstructure parameters that are relevant for the forming properties of steel.

To evaluate the method, full wave field LUS data has been captured on series of samples of different steel grades after hot-rolling, supplied by ArcelorMittal and Tata Steel. To investigate anisotropy, data has been recorded both in the rolling direction (RD) and transverse direction (TD). The data has been inverted to extract parameters having, according to theoretical considerations, increased sensitivity to the (anisotropy in the) forming properties.

2. Wave mode interpretation

From the literature it is known that the frequency-dependent attenuation is related to grain size. Lévesque (1) showed on thick walled steel that attenuation can be related to grain size via an empirical calibration curve. Their measurements were performed on coarse grain austenitic steel. However, for inline monitoring of fine grained material there are two complications. The samples are much thinner, meaning that the scatter signals and coherent reflection are difficult to discriminate. Moreover, the shear wave scattering dominates and will affect the attenuation measurement of the compressional wave, as can be seen in Figure 1b. These two aspects are expected to cause significant uncertainty. Therefore a different approach is followed here.

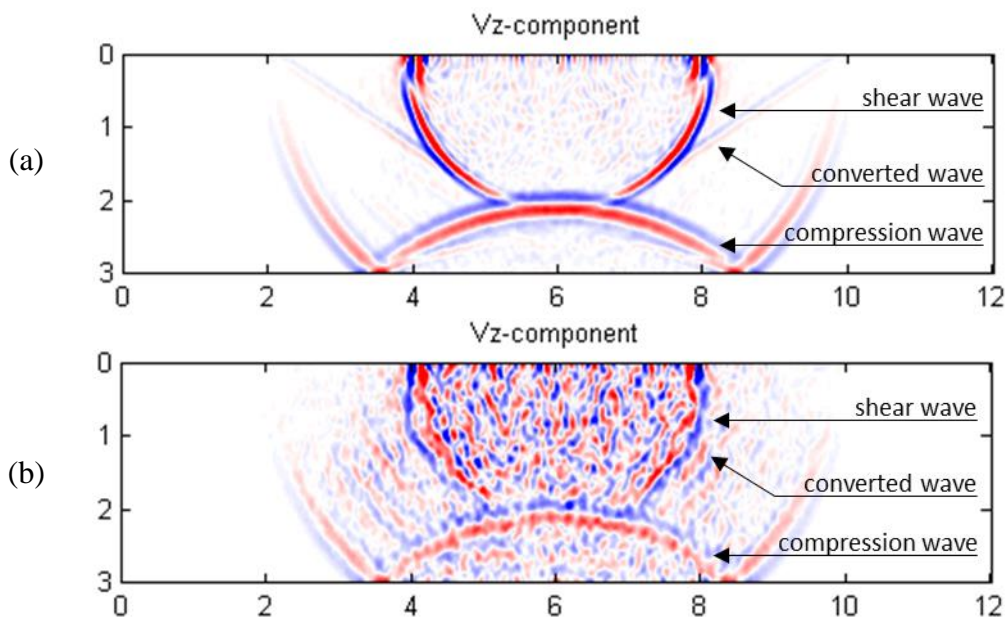


Figure 1. Snapshot from a simulation, at $0.7 \mu\text{s}$ after a pulse at the surface of the sample. The vertical particle velocity is shown for a sample with an average grain size of $5 \mu\text{m}$ (a), and of $50 \mu\text{m}$ (b). The horizontal and vertical axes denote distances in mm. Denoted are the first pressure waves, compressional waves and a mode converted wave.

It is proposed to record the wave field along a line at the bottom surface, i.e. along the bottom line of the samples in Figure 1. The recorded wave field in the space-time domain can be transformed to the wavenumber-frequency domain. In this domain, the different wave modes that propagate in the plate can be distinguished, essentially solving the undesired interference of compressional and shear waves. Then the amplitude along a wave mode can be used as measure for grain size.

The main objective here is to calculate the location of the wave modes in the wavenumber-frequency domain. The first signal arriving after a pulse at the top surface has encountered a single propagation W_p . The second signal arriving, has undergone a propagation downwards, a reflection at the bottom wall, a propagation upwards, a reflection R at the top wall, and again a propagation downwards. Each next signal has an additional set of two reflections (bottom wall and top wall) and two propagations (upwards and downwards). Assuming that propagation upwards and downwards are equal, and that the reflections at the top and bottom walls are equal, all these echoes form an infinite series:

$$A = W_p + W_p(W_p R)^2 + W_p(W_p R)^4 + \dots = W_p \sum_{n=0}^{\infty} (W_p^2 R^2)^n. \quad (1)$$

This series has the exact solution

$$A = W_p \frac{W_p^2 R^2}{1 - W_p^2 R^2}. \quad (2)$$

The propagation operator of the compressional waves (P-waves) reads

$$W_p = e^{-jk_{z,p}d}, \quad (3)$$

where $k_{z,p}$ is the vertical wave number, and d is the propagation distance, i.e. the thickness of the sample.

The denominator of equation (2) determines when interference maxima occur in the wavenumber domain. It turns out that maxima occur when the following condition is satisfied:

$$2m\pi = 2dk_{z,p} = 2d \sqrt{\frac{\omega^2}{c_p^2} - k_x^2}, \quad (4)$$

where ω is the angular frequency, k_x is the horizontal wavenumber, m is the mode number and c_p the compressional wave velocity. For shear waves (S-waves), the same reasoning can be applied, but with subscripts 's' instead of 'p', leading to

$$2m\pi = 2d \sqrt{\frac{\omega^2}{c_s^2} - k_x^2}. \quad (5)$$

The location of each of the compressional and shear wave modes can now be predicted, as curves in the (k_x, k_z) -domain, given their mode number m , the sample thickness d , and the wave velocities, respectively c_p and c_s .

3. Texture characterization

Since the wave mode locations depend on physical sample properties as wave velocities and dimensions, these have to be known sufficiently accurate. In order to obtain those, a series of arrival times of eight compressional wave fronts are tracked in the recorded data (see Figure 2a). These arrival times of the different wave modes are hyperbolically shaped, and can be fitted with an anisotropic hyperbola, mathematically expressed as

$$t_m(x) = \sqrt{(x - x_0)^2 + y_0^2 + (2m + 1)^2 d^2} / c_p(x) + t_0, \quad (6)$$

with Thomsen's weak anisotropy approximation

$$c_p(x) = c_p^{(0)}(1 + \delta \sin^2 \theta \cos^2 \theta + \varepsilon \sin^4 \theta), \quad (7)$$

$$\theta = \tan^{-1}((x - x_0)/d), \quad (8)$$

where the estimated parameters are spatial offsets x_0 and y_0 in two directions, a temporal offset t_0 , and the sample thickness d , the isotropic wave velocity $c_p^{(0)}$ and the anisotropy parameters δ and ε , following Thomsen (2).

The calculated locations of pure P- and S-wave modes are shown in Figure 2b, which match nicely with the locations observed in the data. Note that there are also modes with a mixed character (as e.g. the mode conversion wave shown in Figure 1), which interfere with the pure wave modes, but are ignored in this approach. Once the wave mode location is known, it is possible to integrate the mode energy and display the energy as function of frequency and mode number. By integrating over frequency, only a single value per mode order is obtained.

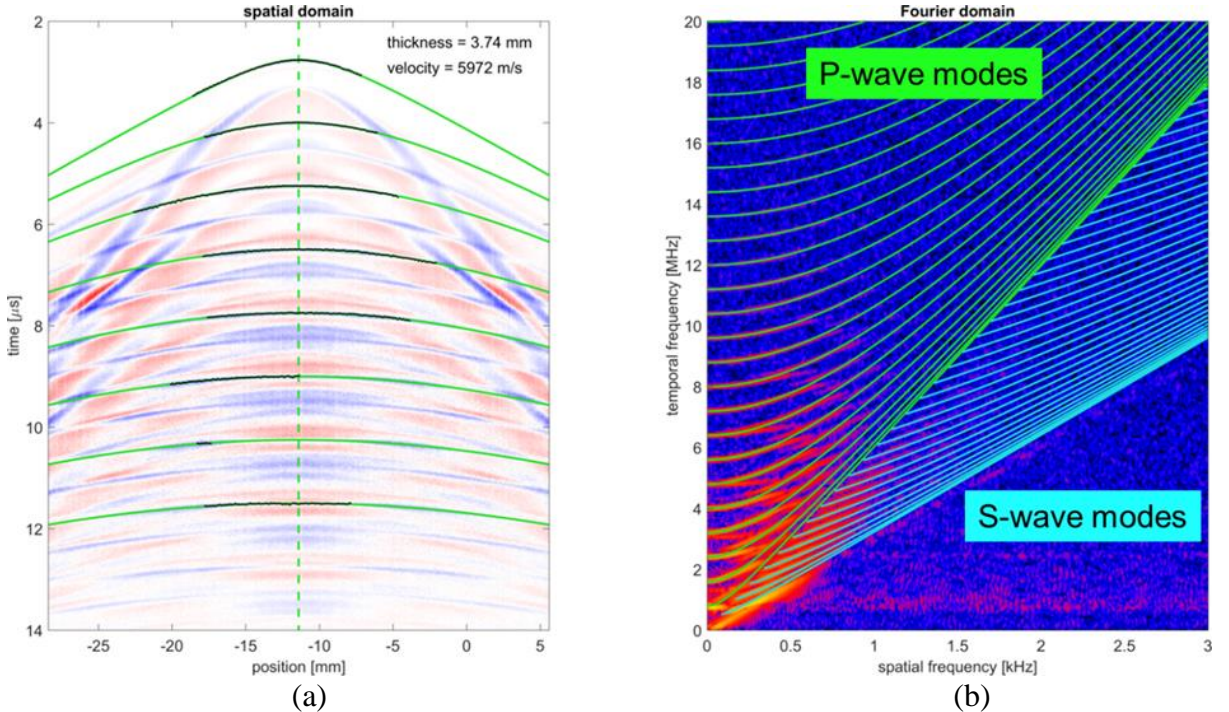


Figure 2. (a) Recorded data, with tracked compressional waves (black) and overlaid hyperbola estimations (green), which provide an estimation for the sample thickness and compressional wave velocity. (b) The locations of the P-wave modes and S-wave modes, based on the estimated sample parameters, superimposed on the Fourier transformed data (red-blue intensity graph).

4. Experimental set-up

A laser ultrasonic setup as shown schematically in Figure 3 has been used to record the ultrasonic wave field along a line at the bottom of the sample, opposite to the generation spot. A Q-switched Nd:YAG pulse laser has been used to generate the ultrasound well within the ablation regime, using suitable optics to focus the laser down to a spot size of 1.7 mm.

The detection side has been powered by a 5 W continuous wave laser which has been delivered to the detection head through a 50 μm multi-mode fibre, resulting in a detection spot size of 0.6 mm when focussed onto the sample. The reflecting light has been collected into a large diameter optical fibre and delivered to a 500 mm scanning confocal Fabry-Pérot interferometer (FPI) for demodulation.

A proprietary control scheme has been used to dynamically lock the FPI to the frequency of the detection laser (3).

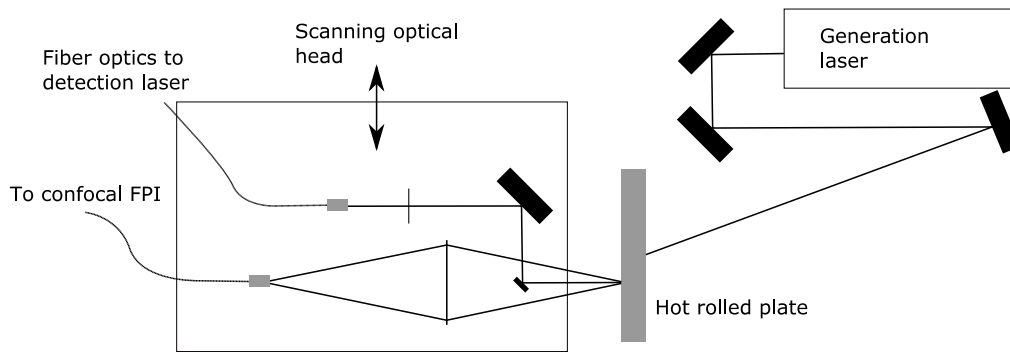


Figure 3. Simplified representation of the laser ultrasound setup with its optical detection head mounted on a linear axis (4).

5. Results

LUS data has been acquired for various steel types from two manufacturers (Arcelor-Mittal and Tata Steel), and in two perpendicular directions (rolling direction, RD, and transverse direction, TD). For each of the data sets, anisotropic hyperbolas are fitted to the data in the spatial-temporal domain, leading to a set of measurement-related parameters (2D spatial offsets x_0 and y_0 , and a temporal offset t_0), and four sample-related parameters (sample thickness d , isotropic wave velocity $c_p^{(0)}$ and anisotropy parameters δ and ε).

Results of two Tata Steel micro-alloy samples are shown in Figure 4. The LUS data has been recorded on each sample in the aforementioned directions. The arrival times of the wave fronts have been identified in the data, and anisotropic hyperbolas have been fitted, following equations (6)-(8). The corresponding velocities are shown in two different representations in the same figure. These anisotropic wave velocities show the sound wave velocities under an angle with respect to the normal, where 0° is perpendicular

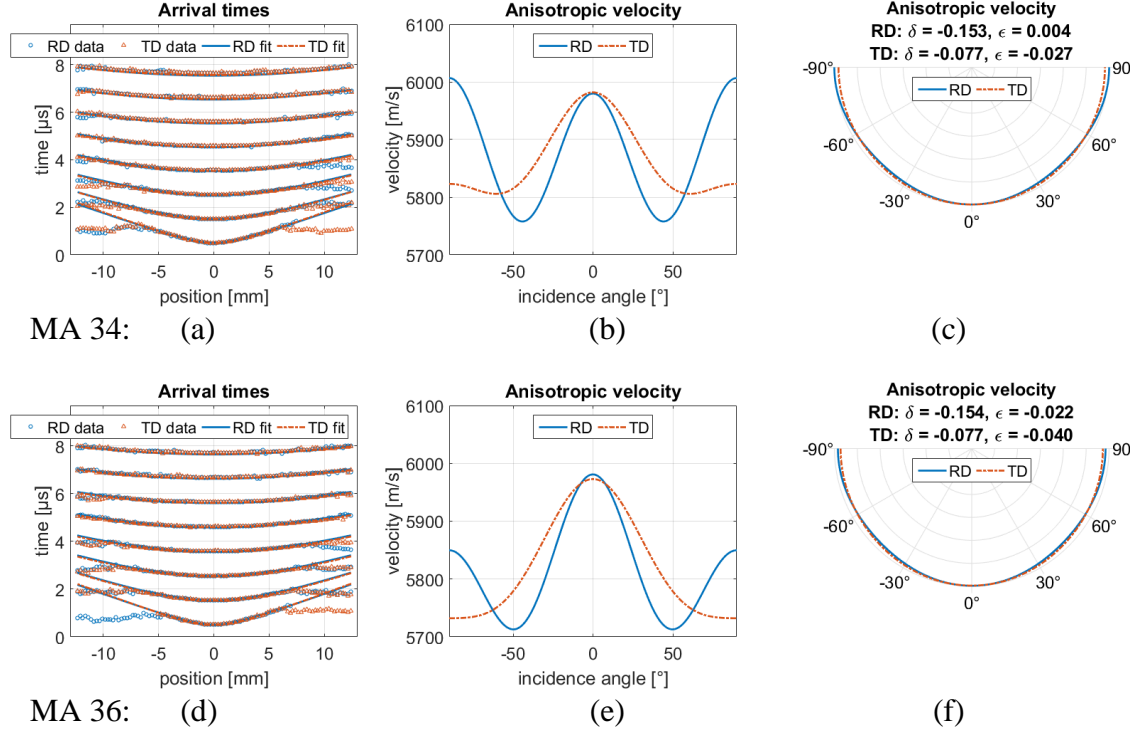


Figure 4. Results from two Tata Steel MA samples: (a) and (d) the picked data points of arriving wave fronts and fitted anisotropic hyperbolas in two directions (rolling direction and transverse direction), (b) and (e) the corresponding anisotropic velocities as function of incidence angle, and (c) and (f) the same velocities displayed in a polar plot.

through the sample and 90° along the surface. In the perpendicular direction the velocities of both measurement directions should be identical, although small deviations can be observed. The velocity profile is different in the two directions, indicating that this anisotropic sound velocity can be used as a metric for the texture of the sample. Note that this metric is less sensitive to grain size, since it uses the arrival times of the fastest wave fronts, which are unaffected by scattering due to grains.

Next, the spatial-temporal data can be Fourier transformed to the $f-k_x$ domain. Using the estimated wave velocity and sample thickness, the individual wave modes in the 2D frequency domain can be located, and the energy along these modes in the $f-k_x$ domain is obtained by integration, as shown in Figure 2.

Per sample, the weighted average energy mode N_{wa} of all N wave mode energies can be obtained as

$$N_{wa} = \frac{\sum_{n=1}^N n E(n)}{\sum_{n=1}^N E(n)}, \quad (6)$$

where $E(n)$ is the energy per wave mode n . In this representation, a low value means that most of the energy is contained in the lower wave modes (i.e. in the lower frequencies).

Since grain size is known to affect the signal in such a way that higher frequencies are more suppressed for larger grains, this means that the weighted average energy mode

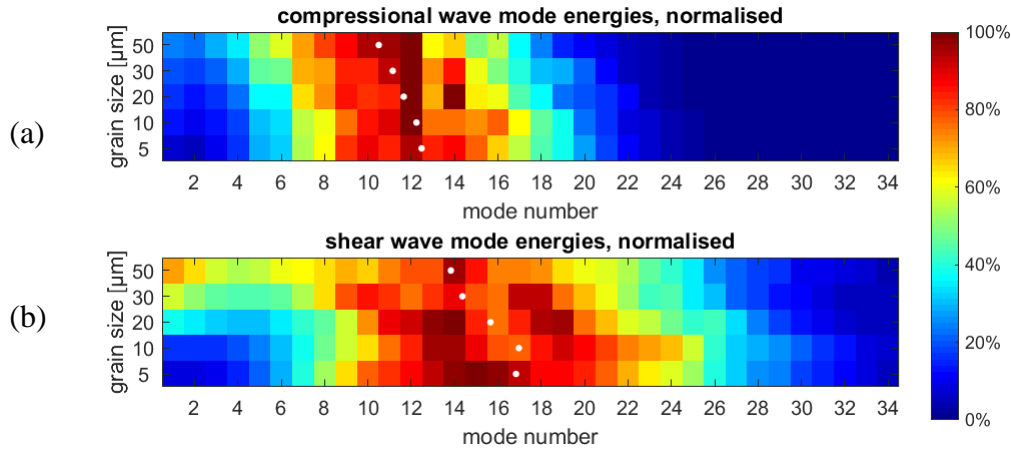


Figure 5. The wave mode energies, as function of mode number (horizontal) and grain size (vertical), obtained from numerical simulations. On top (a), the P-wave modes, and on the bottom (b), the S-wave modes. In both figures, the weighted average energy mode is shown as white dots.

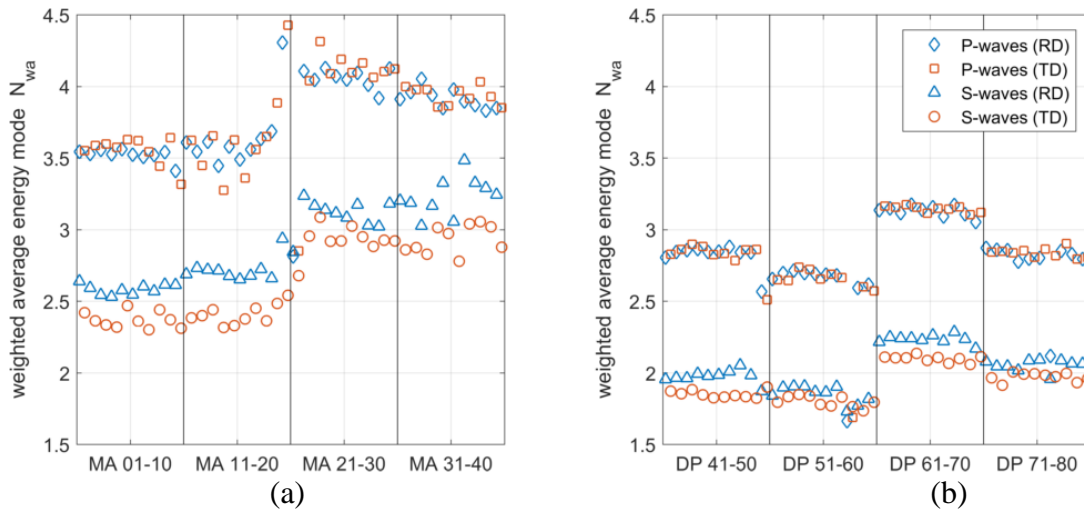


Figure 6. The weighted average energies of four sets of Arcelor-Mittal samples: (a) four sets of micro-alloy steel (MA), and (b) four sets of dual phase steel (DP). For each sample, four energies are shown: P-waves in the rolling direction (RD), P-waves in the transverse direction (TD), and S-waves in the rolling and transverse directions.

decreases with grain size. This is illustrated in Figure 5 for numerical simulation data. Therefore, this metric can be used as a parameter in monitoring grain size.

Some results for eight sets of steel samples are shown in Figure 6: four micro-alloy steel sets and four dual phase steel sets, each consisting of 10 samples. Weighted average energy modes from measurements in two directions (the rolling direction and the transverse direction), and from both P-waves and S-waves are shown. Note that the magnitudes and ratio of P- and S-wave N_{wa} is not comparable due to different excitation sources. The differences between and within sets can be seen. S-waves measured in the transverse direction lead to consistently lower values than in the rolling direction, while for P-waves the values are more or less equal for both directions. Within a given set, variations are more pronounced in the micro-alloy samples than in the dual phase samples. The weighted average energy mode can be used as a metric for the grain size of

the sample. This metric is less sensitive to texture: variations in texture (i.e. in anisotropic velocity profiles), lead to small changes in the location of the wave modes in the f - k_x domain. However, since integration along wave modes occurs in a region around the predicted location, these textural mode location differences will be lost in the integration.

7. Conclusion

The method in this paper shows the potential of LUS data inversion in characterizing sheet metal microstructure. Sample parameters as thickness and anisotropic sound wave velocity can be obtained by fitting anisotropic hyperbolas to spatial-temporal LUS data. From the fitted parameters, the anisotropic wave velocity can be derived, i.e. the wave velocity as function of incidence angle. This velocity profile can be a metric to characterize texture. It is only to a lesser extent affected by scattering, and hence less sensitive to grain size.

After Fourier transforming the LUS data to the 2D frequency domain (f - k_x), individual compressional wave modes and shear wave modes can be distinguished. From the estimated sound velocity, the locations of these wave modes can be obtained. Integration along the modes lead to the energy per wave mode. A simple metric based on the weighted average of the energy can be used as a characteristic for the grain size of a steel sample. This metric is less sensitive to texture, since textural variation will be averaged out in the integration.

In this paper, two metrics have been presented which can be used to characterize the microstructure of a steel sample: either texture or grain size. Since these can be applied to data gathered from an inline LUS measurement system, these can be valuable for real-time monitoring of product uniformity.

Acknowledgements

The research leading to these results has received funding from the European Union's Research Fund for Coal and Steel (RFCS) research programme under grant agreement nr. RFSR-CT-2013-00031.

References

1. D. Lévesque, S.E. Kruger, G. Lamouche, R. Kolarik, G. Jeskey, M. Choquet, and J.-P. Monchalain, *Thickness and grain size monitoring in seamless tube-making process using laser ultrasonics*, NDT & E International, volume 39, issue 8, pages 622-626, 2006
2. L. Thomsen, *Weak Elastic Anisotropy*, Geophysics, volume 51, issue 10, pages 1954-1966, 1986
3. G. J. Deppe, G. Fischer, J. Kowalski, N. Schönartz, inventors; Salzgitter Mannesmann Forschung GmbH, assignee. *Verfahren zur zerstörungsfreien Prüfung von Werkstücken mittels Ultraschall*. German patent DE 102010006922 A1. 2011 Sep 29.
4. D. Krix, R. Schmidt, M. De Soares Silva e Melo Mota, A. Volker, *Laser Ultrasonic Characterisation of Rolled Steel Strip: Wave Propagation in Inhomogeneous Thin Sheets*, 19th World Conference on Non-Destructive Testing (WCNDT), 2016